Electronic Supplementary Material (ESI) for Journal of Materials Chemistry C.

Electronic Supporting Information

Phosphorescent Mechanochromism through the Contraction of $Ag_{12}Cu_2$ Clusters in Tetradecanuclear Copper-Silver Acetylide Complexes

Xu Zhang,[a] Jin-Yun Wang,[a] Di Qiao[a,b] and Zhong-Ning Chen*[a,b]

[a] *State Key Laboratory of Structural Chemistry, Fujian Institute of Research on the Structure of Matter, Chinese Academy of Sciences, Fuzhou, Fujian 350002, China. E-mail: czn@fjirsm.ac.cn*

[b] *College of Chemistry and Materials, Fuzhou Normal University, Fuzhou, Fujian 350007, China*

Table S1. Crystallographic data of the $Ag_{12}Cu_2$ complex **1**.

empirical formula	$C_{222}H_{229}Ag_{12}Cl_2Cu_2O_8P_8$
formula weight	4765.23
crystal system	monoclinic
space group	$P2_1/c$
a (Å)	20.126(4)
b (Å)	48.515(8)
c (Å)	25.912(5)
β (deg)	103.847(3)
V (Å^3)	24566(8)
Z	4
ρ_{calcd} (g/cm^{-3})	1.288
μ (mm^{-1})	1.222
radiation (λ, Å)	0.71073
temperature (K)	293(2)
completeness	99.8
GOF	1.125
R1 (F_o)[a]	0.0676
*w*R2 (F_o^2)[b]	0.2164

[a] $R1 = \Sigma|F_o - F_c|/\Sigma F_o$, [b] $wR2 = \Sigma[w(F_o^2 - F_c^2)^2]/\Sigma[w(F_o)^2)]^{1/2}$

Table S2. The UV-Vis Absorption Spectral Data of $Ag_{12}Cu_2$ Complexes **1–3** in CH_2Cl_2 at Ambient Temperature.

	λ_{abs}/nm (ε/dm^3 mol^{-1} cm^{-1})
1	238 (206937), 253 (163985), 273 (160864), 414 (8731)
2	240 (176105), 247 (179579), 273 (161186), 422 (8278)
3	238 (155491), 249 (129765), 270 (65457), 445 (7963)

Table S3. Partial Molecular Orbital Compositions (%)(%) in the Singlet Excited State for $Ag_{12}Cu_2$ Cluster Complex **2'** in Dichloromethane by TD-DFT Method at the B3LYP Level.

orbital	energy (eV)	MO contribution (%)			
		Cu (s/p/d)	Ag (s/p/d)	$C{\equiv}CC_6H_5$	$P(CH_2PH_2)_3$
LUMO+10	-1.47	9.84 (0/98/2)	31.16 (47/51/2)	55.57	3.43
LUMO+8	-1.63	28.96 (0/99/1)	40.38 (35/64/1)	27.11	3.54
LUMO+5	-1.75	12.44 (1/98/1)	37.43 (79/19/2)	46.23	3.90
LUMO+4	-1.80	22.59 (0/98/2)	42.89 (70/28/2)	31.75	2.77
LUMO+3	-1.82	21.61 (0/98/2)	45.24 (72/27/1)	30.27	2.88
LUMO+2	-1.97	37.63 (0/99/1)	39.94 (27/72/1)	22.03	0.41
LUMO+1	-1.98	37.38 (0/99/1)	40.85 (24/74/1)	21.41	0.36
LUMO	-2.59	32.88 (50/42/8)	36.18 (82/12/6)	26.08	4.85
HOMO	-6.17	18.67 (12/6/82)	14.06 (6/13/81)	42.15	25.11
HOMO-1	-6.22	13.38 (1/58/40)	32.24 (12/37/52)	48.66	5.72
HOMO-2	-6.24	14.67 (0/61/39)	32.90 (11/38/51)	46.94	5.49
HOMO-3	-6.26	9.93 (5/20/75)	22.92 (23/14/63)	50.73	16.43
HOMO-4	-6.32	10.01 (5/23/72)	27.97 (21/19/60)	53.88	8.14
HOMO-5	-6.34	15.75 (17/32/50)	29.84 (8/56/36)	43.68	10.73
HOMO-7	-6.44	14.08 (18/4/78)	21.87 (35/8/57)	49.80	14.26
HOMO-10	-6.64	14.91 (0/11/89)	26.20 (39/12/49)	56.93	1.97
HOMO-13	-6.77	24.39 (0/18/82)	37.34 (32/11/58)	37.24	1.03

Table S4. The Absorption Transitions for $Ag_{12}Cu_2$ Complex **2'** in Dichloromethane by TD-DFT Method at the B3LYP Level.

States	*E*, nm (eV)	O.S.	Transition (Contrib.)	Assignment	Exp. (nm)
S_1	402 (3.09)	0.0209	HOMO→LUMO (93%)	^{1}MC/^{1}LMCT/^{1}IL	422
S_{13}	351 (3.54)	0.0539	HOMO-10→LUMO (45%) HOMO-13→LUMO (40%)	^{1}MC/^{1}LMCT/^{1}IL ^{1}MC/^{1}IL/^{1}LMCT	
S_{22}	328 (3.79)	0.0711	HOMO-3→LUMO+1 (45%) HOMO-2→LUMO+1 (11%)	^{1}LMCT/^{1}MC/^{1}IL ^{1}MC/^{1}LMCT/^{1}IL	
S_{25}	323 (3.83)	0.0742	HOMO→LUMO+3 (44%) HOMO-3→LUMO+2 (9%)	^{1}LMCT/^{1}MC/^{1}IL ^{1}LMCT/^{1}MC/^{1}IL	
S_{27}	322 (3.85)	0.1009	HOMO→LUMO+4 (33%) HOMO-4→LUMO+1 (12%)	^{1}MC/^{1}IL/^{1}LMCT ^{1}LMCT/^{1}MC/^{1}IL	
S_{32}	318 (3.90)	0.1425	HOMO-3→LUMO+3 (15%) HOMO-5→LUMO+2 (11%) HOMO-4→LUMO+3 (9%)	^{1}LMCT/^{1}MC/^{1}IL ^{1}MC/^{1}LMCT/^{1}IL ^{1}MC/^{1}IL/^{1}LMCT	
S_{42}	310 (4.00)	0.1025	HOMO-7→LUMO+2 (19%) HOMO-7→LUMO+1 (12%) HOMO-4→LUMO+4 (10%)	^{1}LMCT/^{1}MC/^{1}IL ^{1}LMCT/^{1}MC/^{1}IL ^{1}MC/^{1}IL/^{1}LMCT	
S_{120}	284 (4.37)	0.1354	HOMO-1→LUMO+10 (14%) HOMO→LUMO+10 (9%) HOMO-7→LUMO+8 (8%)	^{1}IL/^{1}MC ^{1}IL/^{1}MC/^{1}LLCT/^{1}LMCT ^{1}MC/^{1}LMCT/^{1}IL	273

Table S5. Partial Molecular Orbital Compositions (%) in the Lowest Triplet Excited State and the Emission Transitions for $Ag_{12}Cu_2$ Complex **2'** in Dichloromethane by TD-DFT Method at the B3LYP Level.

orbital	energy (eV)	MO contribution (%)			
		Cu (s/p/d)	Ag (s/p/d)	$C{\equiv}CC_6H_5$	$P(CH_2PH_2)_3$
LUMO	-3.33	32.03 (33/52/15)	40.44 (74/14/12)	22.89	4.65
HOMO	-6.17	12.20 (0/76/24)	33.97 (10/42/48)	49.2	4.62
HOMO-1	-6.19	7.72 (2/85/14)	31.71 (8/41/51)	52.46	8.1
HOMO-6	-6.45	21.05 (27/17/57)	16.37 (8/61/31)	36.88	25.7

state	*E*, nm (eV)	O.S.	transition (contrib.)	assignment	exp. (nm)
T_1	562 (2.21)	0.0000	HOMO-6→LUMO (42%) HOMO-1→LUMO (23%) HOMO→LUMO (18%)	^{3}MC/^{3}LMCT/^{3}IL ^{3}MC/^{3}LMCT/^{3}IL ^{3}MC/^{3}LMCT/^{3}IL	566

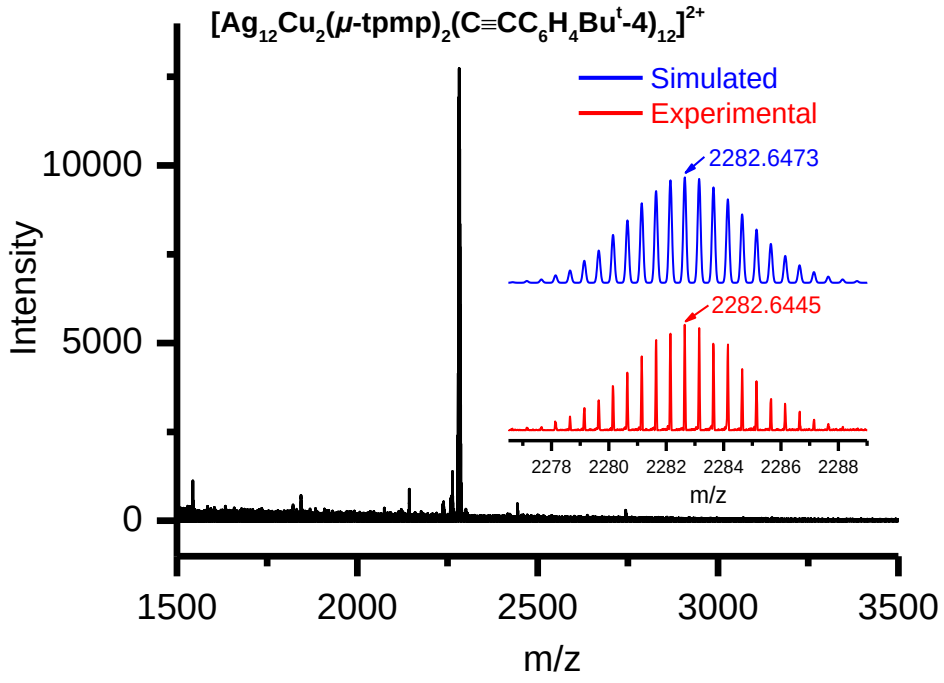

Figure S1. The high resolution mass spectrometry of $Ag_{12}Cu_2$ cluster complex **1**.

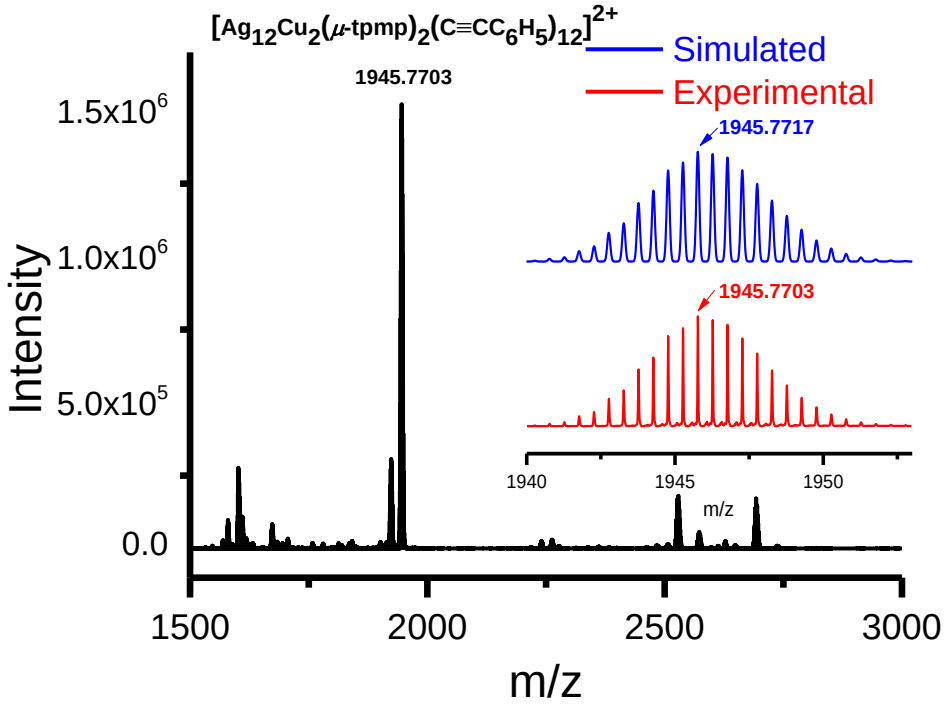

Figure S2. The high resolution mass spectrometry of $Ag_{12}Cu_2$ cluster complex **2**.

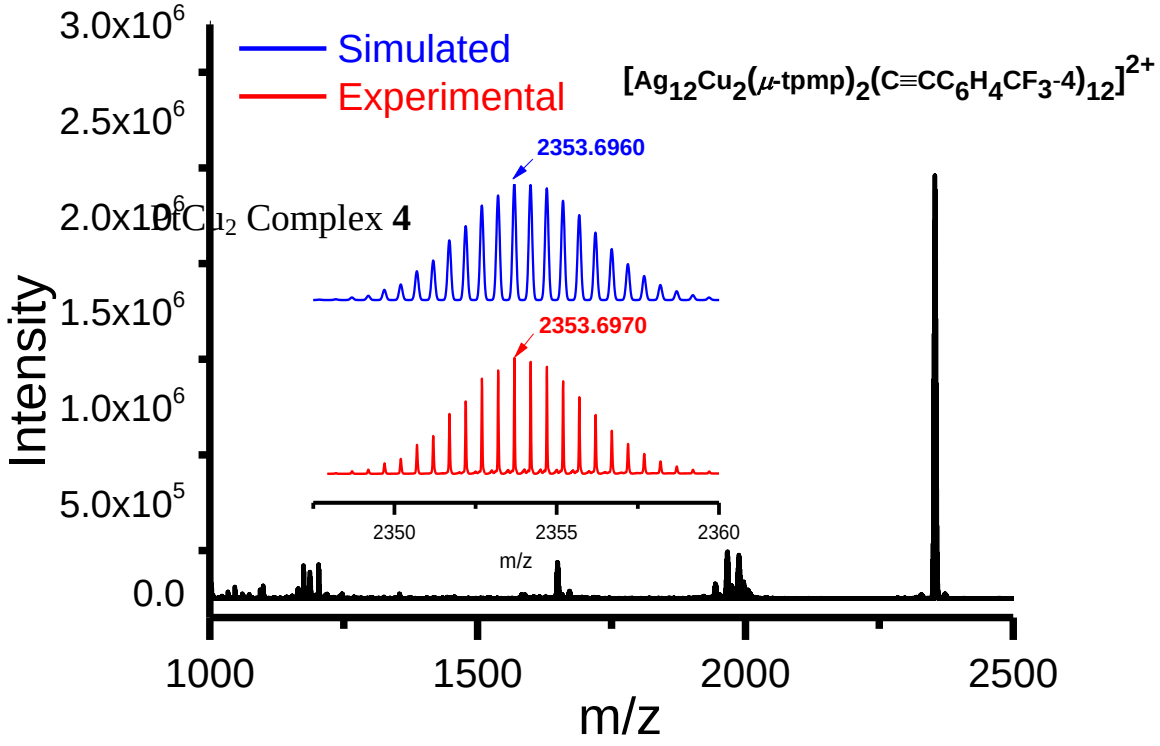

Figure S3. The high resolution mass spectrometry of $Ag_{12}Cu_2$ cluster complex **3**.

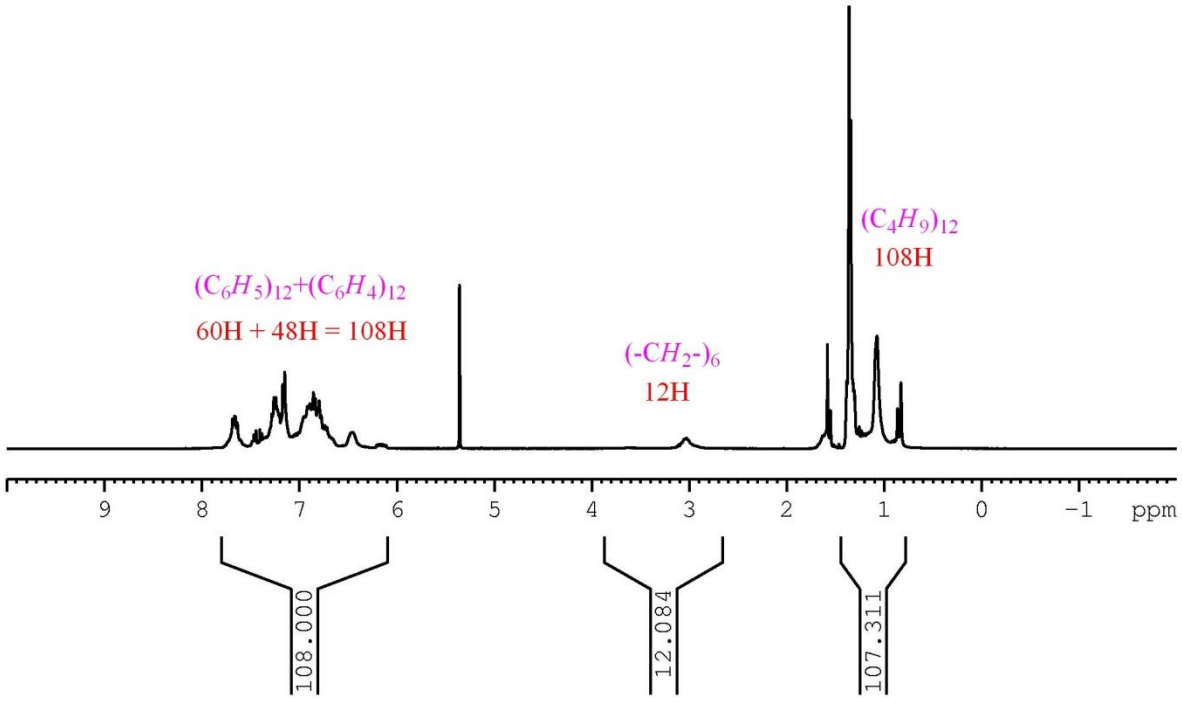

Figure S4. The ^{1}H NMR spectrum of $Ag_{12}Cu_2$ cluster complex **1** in CD_2Cl_2 solution at ambient temperature.

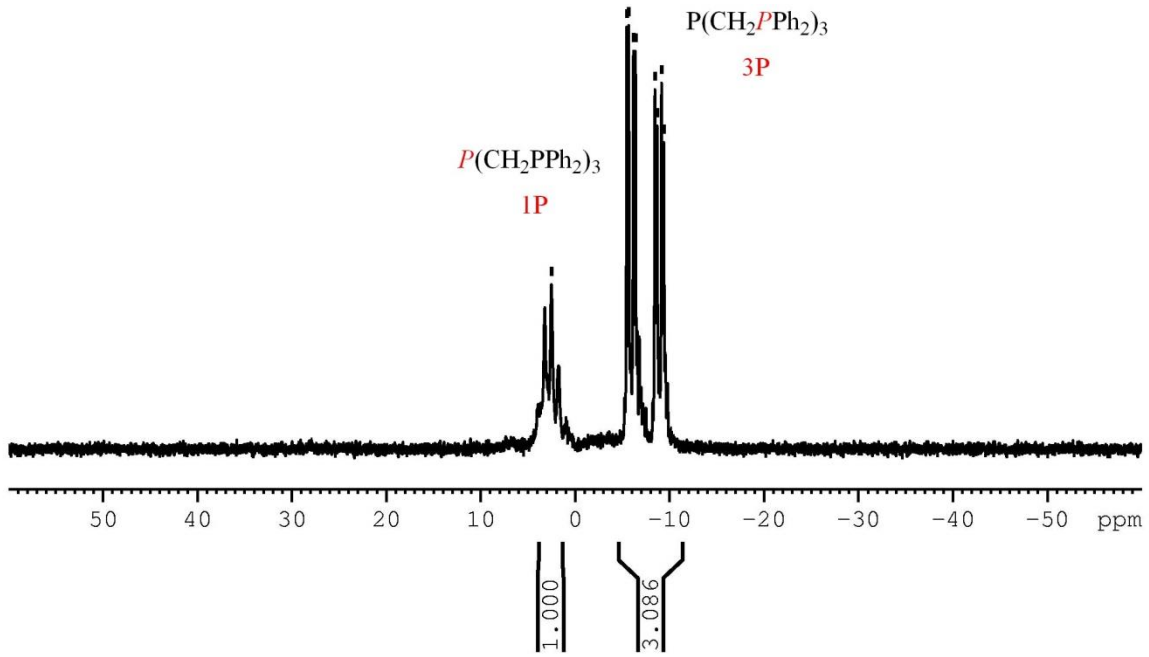

Figure S5. The $^{31}P\{^{1}H\}$ NMR spectrum of $Ag_{12}Cu_2$ cluster complex **1** in CD_2Cl_2 solution at ambient temperature.

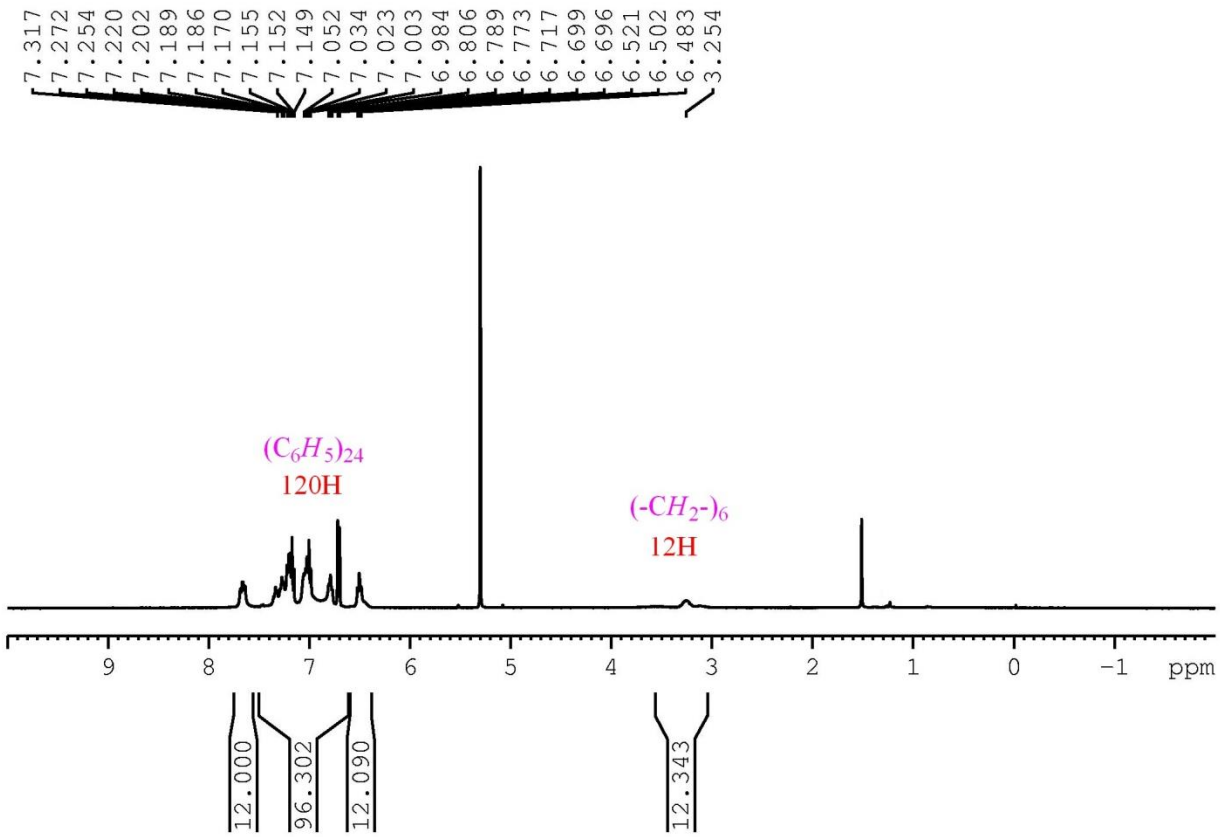

Figure S6. The ^{1}H NMR spectrum of $Ag_{12}Cu_2$ cluster complex **2** in CD_2Cl_2 solution at ambient temperature.

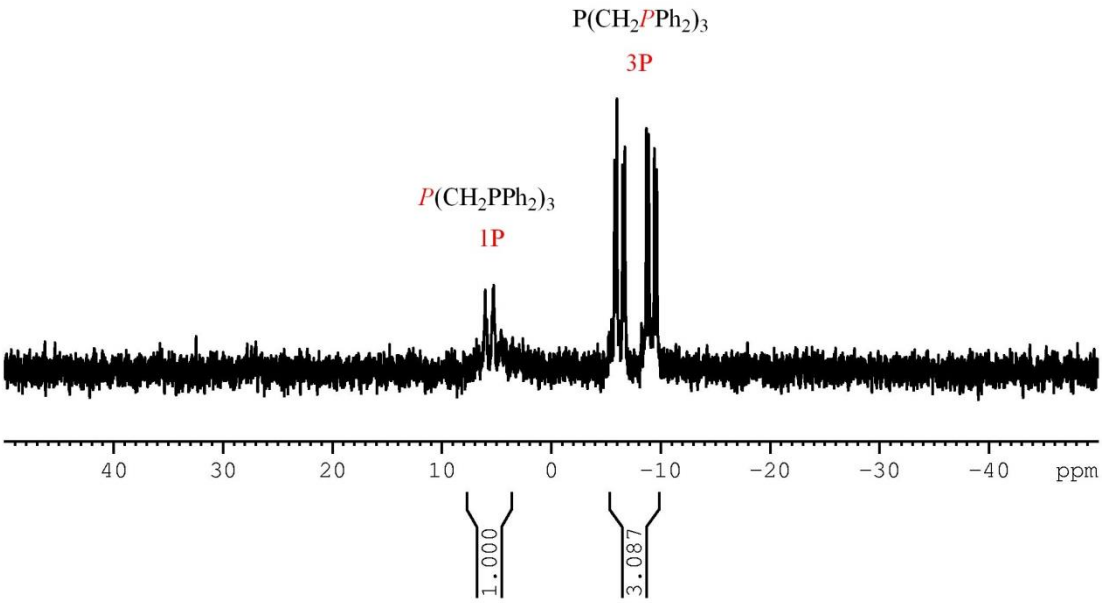

Figure S7. The $^{31}P\{^{1}H\}$ NMR spectrum of $Ag_{12}Cu_2$ cluster complex **2** in CD_2Cl_2 solution at ambient temperature.

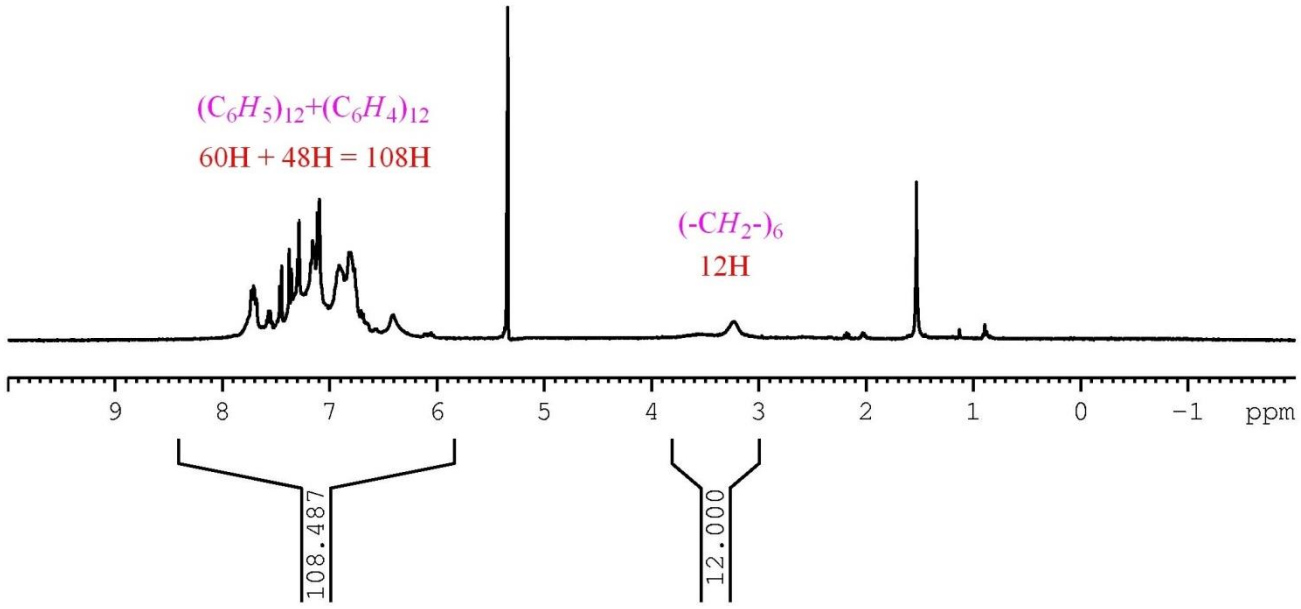

Figure S8. The ^{1}H NMR spectrum of $Ag_{12}Cu_2$ cluster complex **3** in CD_2Cl_2 solution at ambient temperature.

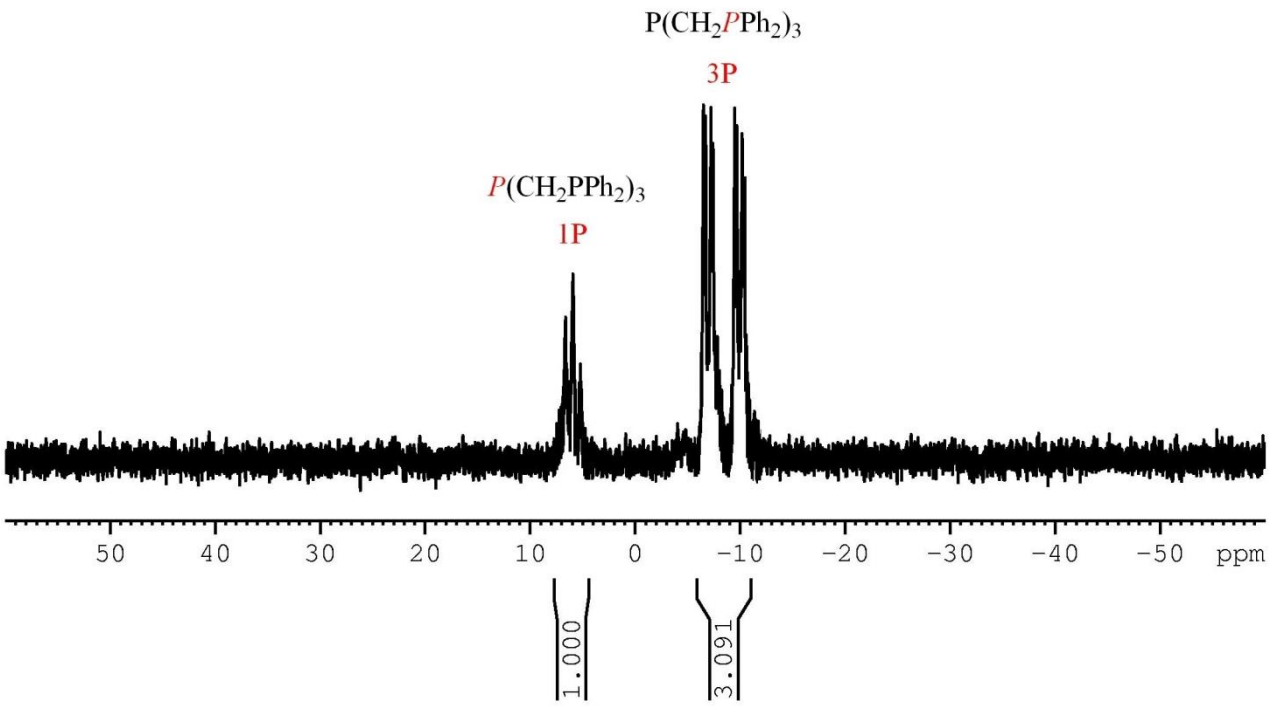

Figure S9. The $^{31}P\{^{1}H\}$ NMR spectrum of $Ag_{12}Cu_2$ cluster complex **3** in CD_2Cl_2 solution at ambient temperature.

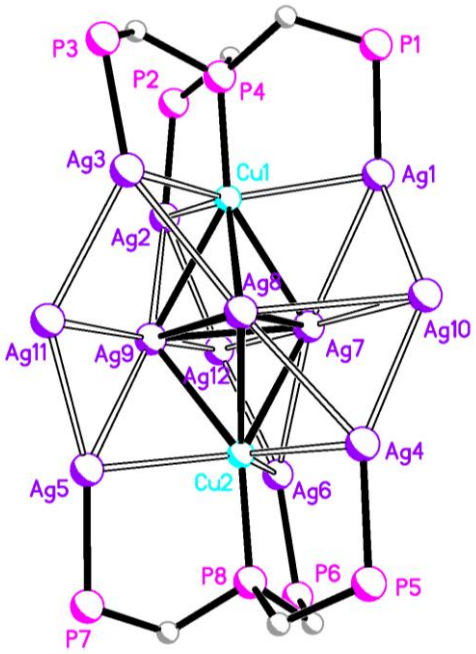

Figure S10. A view of $Ag_{12}Cu_2$ cluster structure in complex **1** with atom labeling scheme. Phenyl groups on P atoms and 4-tert-butylbenzeneacetylides are omitted for clarity.

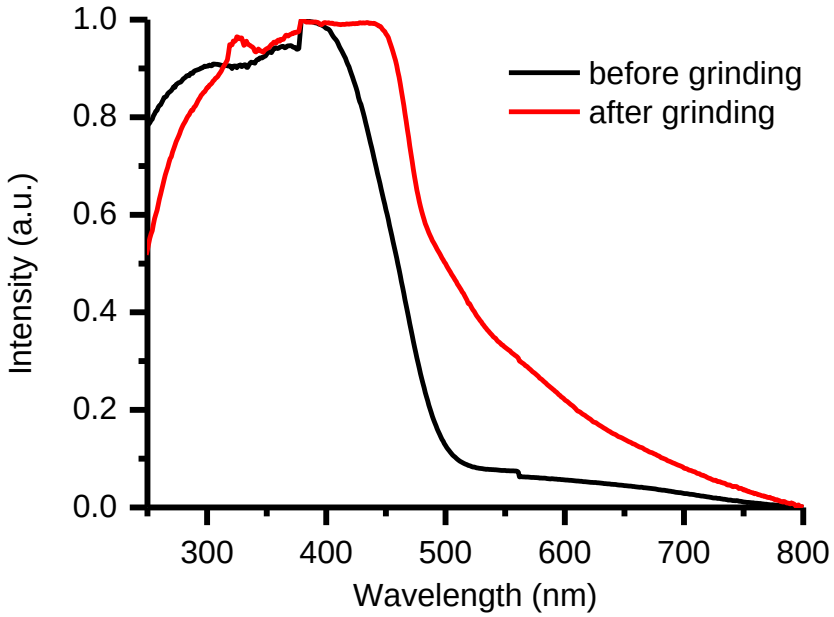

Figure S11. The solid-state UV-Vis spectra of $Ag_{12}Cu_2$ cluster complex **1** before and after mechanical grinding.

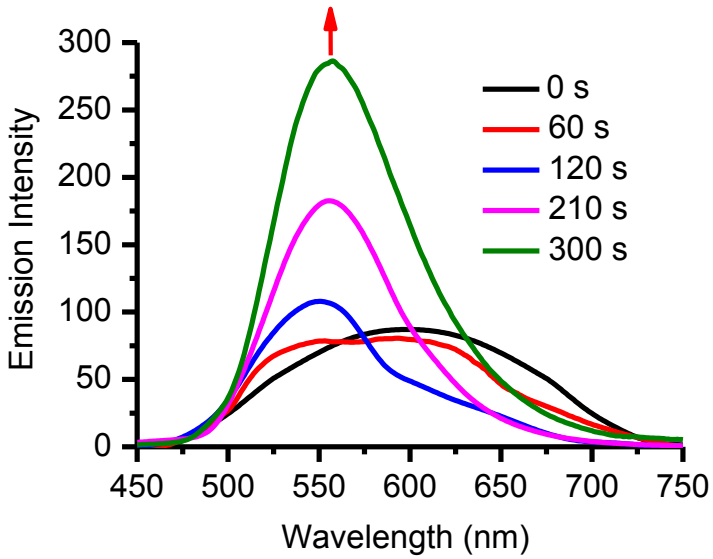

Figure S12. Phosphorescent emission spectral changes of the ground species for $Ag_{12}Cu_2$ cluster complex **1** upon exposure to CH_2Cl_2 vapour, showing the gradual restoration to the original state.